

Studies on structural, optical and magnetic properties of (Ru, Mn) codoped ZnO nanostructures

K R Aranganayagam¹, S Senthilkumaar² and N Ganapathi Subramaniam³

¹Department of Chemistry, Kumaraguru College of Technology, Coimbatore -641049, Tamilnadu, India

²Advanced Materials Research Laboratory, Department of Chemistry, PSG College of Technology, Coimbatore – 641004, Tamilnadu, India

³Quantum Functional Semiconductor Research Centre (QSRC), Dongguk University-Seoul, Seoul, South Korea

E-mail: aranganayagam@gmail.com

Abstract. Ruthenium and manganese codoped ZnO ($\text{Ru}_x\text{Mn}_{0.01}\text{Zn}_{0.99-x}\text{O}$; $x = 0.01, 0.02$ and 0.03) were synthesized by sol-gel method via ultrasonication. The effects of codoping on structural, microstructural, optical and magnetic properties of the as-synthesized materials were characterized through X-ray diffraction (XRD), high resolution scanning electron microscopy (HRSEM), high resolution transmission electron microscopy (HRTEM), energy dispersive X-ray spectroscopy (EDS), photoluminescence (PL) and SQUID magnetometer, respectively. From the XRD pattern, it is evident that all the diffraction peaks can be indexed to the hexagonal wurtzite structure and shows the incorporation of dopants i.e. Ru and Mn are substituted in the ZnO lattice. Nanosphere like morphology was observed in HRTEM analysis and the average particle sizes are found to be 20-30 nm, which are good agreement with the XRD crystallite size by Scherrer formula. Photoluminescence (PL) studies were carried out to investigate the optical properties of the as-synthesized materials and the defects related strong green emission peaks was observed in the TM codoped ZnO samples. It can be clearly seen from SQUID results, the loop is linear with the field indicating the presence of paramagnetism / anti ferromagnetism in the samples.

1. Introduction

One of the well known materials in metal oxide family is zinc oxide (ZnO), because of their wide band gap ($E_g = 3.2$ eV) with a large binding energy (60 meV). Also zinc oxide based nano materials are excellent thermal and chemical stability, especially in optoelectronic and magnetic properties this can be used for the wide range high technology applications [1]. Zinc oxide based research has continued may decades to tune the material properties. In addition to that transition metals (TM) into zinc oxide either the way of doping / codoping has proved to enhance optical and magnetic properties. In particularly, divalent TM in ZnO dilute magnetic semiconductors (DMS's) has been extensively studied and mostly reported their ferromagnetism (FM) behaviour over different dopants [2-6]. Recently, researchers are showing their interest towards the different applications on codoping systems. Wei *et al* [7] reported the room temperature (RT) ferromagnetism of (Co, Cu) codoped ZnO and the magnetization increases with increasing concentration of Cu. Similarly, the magnetic behaviors of Ni and Mn codoped ZnO were studied by Vijayaprasath *et al* [8] and it exhibits ferromagnetism with higher magnetization when compared with pure Ni doped and Mn doped ZnO.



The highly oriented c-axis wurzite structure and RT ferromagnetism with large positive magnetoresistance was observed by Gu *et al* [9]. Magnetic behaviour of Co-Mn codoped ZnO were reported [10] and the FM increases with the concentration of Mn increases. The FM interaction in DMS is accounted for spin polarized electrons with free carriers. Interestingly, super paramagnetic and RTFM behaviour was observed in Fe/Co co-doping in ZnO. The change in the FM to super paramagnetic nature may be due to the super exchange interaction between the dopants and ZnO [11]. From the literature survey, it is understood that divalent codoping systems were studied extensively and limited reports are available on trivalent doping systems.

Several methods were available to syntheses these kind of materials like chemical vapour deposition, hydrothermal, sonochemical, co-precipitation, sol-gel, microbial process etc. Among these, sol-gel method is a simple, inexpensive and versatile route to syntheses ZnO based materials. Our research group, focused on material characterizations and its applications of ZnO based material [12, 13]. In this paper, an approach with two different TMs on host ZnO lattices ie. trivalent Ru ion and divalent Mn are expected to bring interesting results. The main purpose of adding Ru^{3+} is to significantly influence the optical and magnetic properties of ZnO and also ruthenium is the metal which can exist eight different oxidation states. This may play an important role to create some new magnetic materials in future spintronics device applications. To understand the effect of codoping on ZnO, attempts were made to syntheses pure ZnO and (Ru, Mn) codoped ZnO nanostructures by sol – gel method via ultrasonication and characterized.

2. Materials and methods

2.1. Synthesis of ZnO and (Ru, Mn) codoped ZnO

The precursor sols were prepared from zinc acetate dihydrate ($\text{Zn}(\text{CH}_3\text{COO})_2 \cdot 2\text{H}_2\text{O}$), was dissolved in aqueous ethanol (1:1). The desired concentration of dopants trihydrated ruthenium trichloride ($\text{RuCl}_3 \cdot 3\text{H}_2\text{O}$; 1, 2 and 3 mol%) and dihydrated manganese chloride ($\text{MnCl}_2 \cdot 2\text{H}_2\text{O}$; 1 mol%) were added drop-wise to the zinc acetate solution and stirred at 50°C for 6h to achieve desired stoichiometry. The resultant product were dried and calcined at 500°C for an hour to get a ZnO and $\text{Ru}_x\text{Mn}_{0.01}\text{Zn}_{0.99-x}\text{O}$ where, $x = 0.01, 0.02$ and 0.03 .

2.2. Characterization techniques

The crystallographic studies of ZnO and (Ru, Mn) codoped ZnO nano structures were analyzed by Shimadzu XRD – 6000 X-ray diffractometer with $\text{CuK}\alpha$ radiation. Micro structural characterization at high magnifications was carried out using high resolution scanning electron microscope (HRSEM, FEI Quanta FEG 200), high resolution transmission electron microscope (HRTEM, JEOL JSM 200) and the elemental compositions were obtained by energy dispersive X-ray spectrophotometer (EDX). The UV-Vis. absorption spectra were recorded using Shimadzu UV-1600 spectrometer (200-800 nm). The photoluminescence (PL) spectra were obtained by Flurolog spectro fluorometer with the excitation of 380 nm. Magnetic properties were studied using Semiconducting Quantum Interface Device (SQUID) magnetometer.

3. Results and discussion

3.1 Structural and micro structural studies

The XRD pattern of ZnO and (Ru, Mn) codoped ZnO are shown in the figure 1 (a, b). All the samples are shows the perfect orientation (100), (002), (101) and it is evident that all the diffraction peaks can be indexed to the hexagonal wurzite structure (JCPDS: 89-1397). There is no evidence for the secondary phase upto the concentration 0.02 shows the incorporation of Ru and Mn are substituted in the ZnO lattice and the substitutions and are not disturbing the hexagonal wurzite structure. When the concentration of Ru reaches to 0.03 some extra peaks was observed. The Observed secondary phases are due to the formation of RuO_2 , Mn_2O_3 , ZnMnO_3 (supported by JCPDS data).

It is further confirmed by the change in the value of lattice parameters, crystallite size and the volumes of the unit cell are presented in table 1. The lattice constants a and c of wurtzite ZnO were calculated according to the Bragg's law, $n\lambda = 2d\sin\theta$. For hexagonal structure of ZnO, lattice a and c given by

$$\left[\frac{1}{d^2} = \frac{4}{3} \left\{ \frac{h^2 + hk + k^2}{a^2} \right\} + \frac{l^2}{c^2} \right] \quad (1)$$

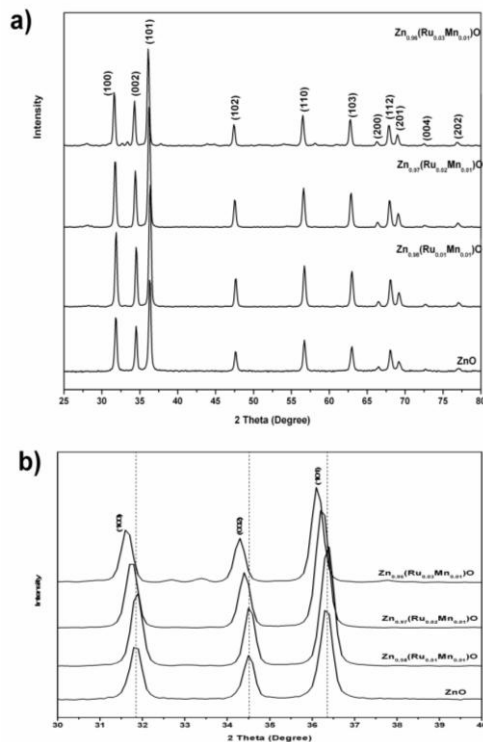


Figure 1. a) XRD pattern of ZnO and (Ru, Mn) codoped ZnO; b) expanded XRD pattern.

for the (100) orientation, the lattice constant a was calculated by $a = \frac{\lambda}{\sqrt{3}\sin\theta}$. For the (002) orientation, the lattice constant c was calculated by $c = \frac{\lambda}{\sin\theta}$.

Volume of the unit cell gradually increases with the concentration of Ru increases. At the same time the relative intensity of the XRD peak increases with the Ru concentration increases. The well defined Bragg peak indicates the good crystallinity of the sample. The concentration increases, the peak (100), (002), (101) are shifted to the lower angle (figure 1 b) and the average crystallite size were calculated using Debye Scherrer formula and it is found to be in the range of 25 – 29 nm. The increasing value in the crystallite size and volume of the unit cell is due to the ionic radius of dopants, Mn (0.80) and Ru (0.77) is slightly higher than that of the host Zn (0.74).

Table 1. XRD and EDS data for ZnO and (Ru, Mn) codoped ZnO.

Samples	Crystallite size (nm)	Lattice parameters (for hexagonal, $a=b \neq c$)		Volume of the unit cell (\AA^3)	Elemental composition by EDS analyses (atomic %)			
		a	c		Ru	Mn	Zn	O
ZnO	25.01	3.2450	5.2057	47.47	-	-	65.27	34.73
$\text{Ru}_{0.01}\text{Mn}_{0.01}\text{Zn}_{0.98}\text{O}$	24.99	3.2426	5.2063	47.41	0.64	0.52	48.90	49.95
$\text{Ru}_{0.02}\text{Mn}_{0.01}\text{Zn}_{0.97}\text{O}$	26.60	3.2545	5.2119	47.81	0.96	0.34	44.88	53.82
$\text{Ru}_{0.03}\text{Mn}_{0.01}\text{Zn}_{0.96}\text{O}$	28.98	3.2661	5.1966	48.01	1.18	0.44	46.86	51.53

The morphology of the samples was studied using HRSEM and the images of the synthesized nanostructures are shown in figure 2. As seen from the figures, there is no obvious difference in the powder morphology and found uniformly packed spherical grains indicating the incorporation of Ru and Mn ion on ZnO lattices. The high resolution transmission electron spectroscopy, HRTEM images of ZnO and (Ru, Mn) codoped ZnO are shown figures 3. It reveals from the HRTEM analyses, nanosphere like morphology was observed for the both pure and codoped ZnO crystals. The average particle size of the pure and codoped ZnO are about in the range of 24-30 nm, which are good agreement with XRD crystallite size.

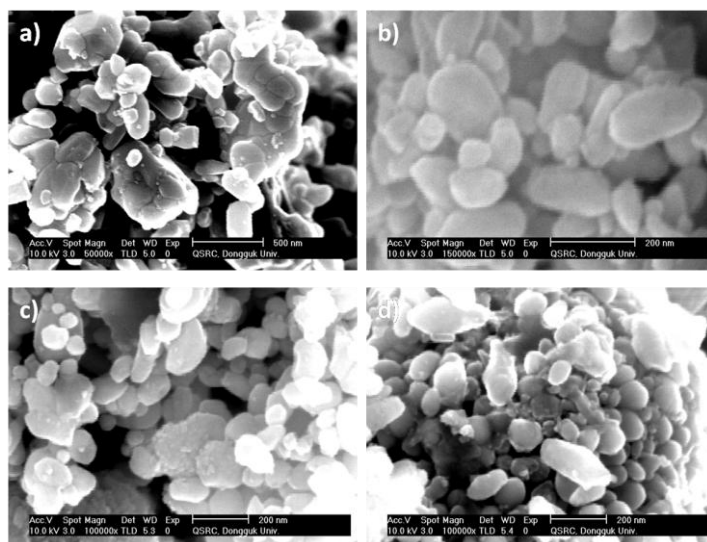


Figure 2. HRSEM image of a) ZnO b) $\text{Ru}_{0.01}\text{Mn}_{0.01}\text{Zn}_{0.98}\text{O}$; c) $\text{Ru}_{0.02}\text{Mn}_{0.01}\text{Zn}_{0.97}\text{O}$; d) $\text{Ru}_{0.03}\text{Mn}_{0.01}\text{Zn}_{0.96}\text{O}$.

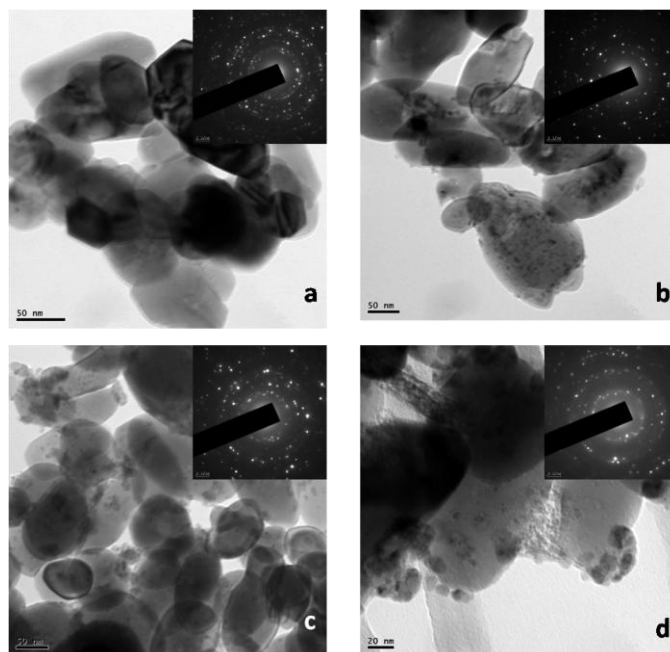


Figure 3. HRTEM image of a) ZnO b) $\text{Ru}_{0.01}\text{Mn}_{0.01}\text{Zn}_{0.98}\text{O}$; c) $\text{Ru}_{0.02}\text{Mn}_{0.01}\text{Zn}_{0.97}\text{O}$; d) $\text{Ru}_{0.03}\text{Mn}_{0.01}\text{Zn}_{0.96}\text{O}$.

3.2 Optical Properties

In order to understand the optical properties of ZnO and (Ru, Mn) codoped ZnO, UV-Vis and photoluminescence (PL) studies were carried out at room temperature. From the UV-Vis spectra, the photon energy (eV) dependent optical absorption spectra, the direct band gap of the synthesized materials are increases (3.31 eV) upto the Ru concentration (0.02) and then it gradually decreases (3.24 eV) with increasing concentration of Ru reaches 0.03. The absorption peaks shifted to the longer wave length with increasing Ru concentration. The shift of wavelength is due to the lattice distortion was takes places upon doping of Ru and Mn into the ZnO lattice. PL spectra of ZnO and (Ru, Mn) codoped ZnO are shown in the figures 4. It is well known that, the ZnO nano crystals show the near band edge emission, NBE around 390 nm [14]. The near band edge UV emission to the NBE for the ZnO is originates from the recombination of exciton-exciton energy levels. In codoped ZnO, the defects related strong green emission peaks was observed in the visible range (460 – 480 nm). The defects such as oxygen vacancies (VO^\cdot) [15] and the zinc interstitials (Zn_i) are responsible for the green emission in ZnO [16]. With the incorporation of Ru at 0.02, the relative band emission intensity increases and then it quenches in further addition. The decrease in the bandgap in the UV-Vis and relative band emission is due to the formation of secondary phases (discussed in XRD).

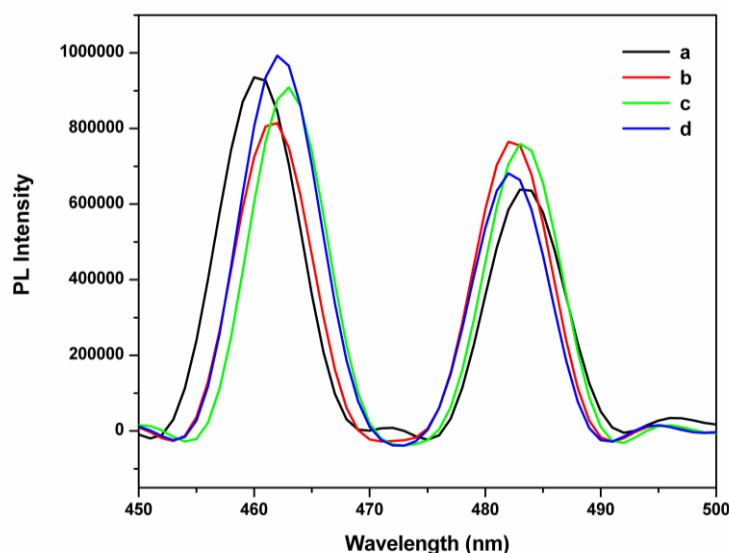


Figure 4. Photoluminescence spectra of a) ZnO
b) $Ru_{0.01}Mn_{0.01}Zn_{0.98}O$; c) $Ru_{0.02}Mn_{0.01}Zn_{0.97}O$;
d) $Ru_{0.03}Mn_{0.01}Zn_{0.96}O$.

3.3 Magnetic Properties

The room temperature magnetic hysteresis loop, $M-H$ curve of (Ru, Mn) codoped ZnO nanostructures and the magnified hysteresis loop are shown in figure 5. It can be clearly seen that the loop is linear with the field indicating the absence of ferromagnetism in the samples. It is observed that decrease in the magnetic moment (emu/g) with increasing concentration of Ru; saturation magnetization is not observed upto the maximum applied field 3000 Oe, as shown in figure 5. The magnetization values observed at 3000 Oe are 8.25, 6.75 and 4.31 emu/g for $Ru_{0.01}Mn_{0.01}Zn_{0.98}O$, $Ru_{0.02}Mn_{0.01}Zn_{0.97}O$ and $Ru_{0.03}Mn_{0.01}Zn_{0.96}O$, respectively. From the magnetic moment it is observed that quenching of antiferromagnetism in the increasing ruthenium concentration. In our previous reports, pure ZnO exhibits ferromagnetic in nature [13], upon codoping of transition metals Ru and Mn in ZnO, the absence of ferromagnetic behaviour was observed.

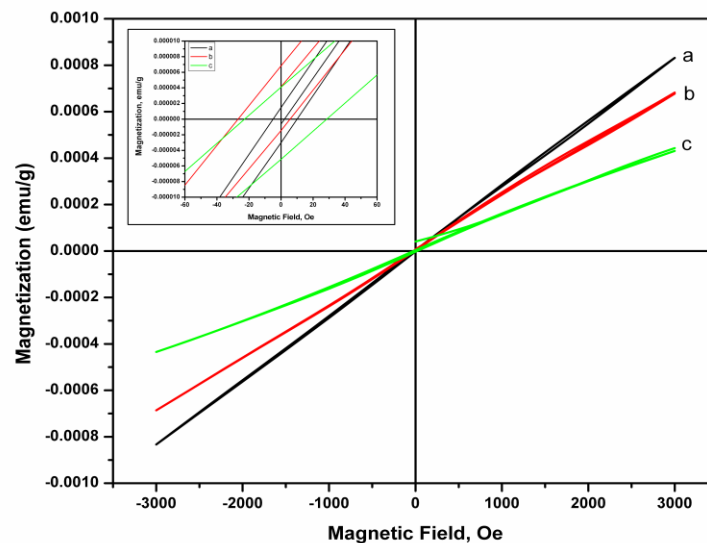


Figure 5. M - H curve of a) $\text{Ru}_{0.01}\text{Mn}_{0.01}\text{Zn}_{0.98}\text{O}$; b) $\text{Ru}_{0.02}\text{Mn}_{0.01}\text{Zn}_{0.97}\text{O}$; c) $\text{Ru}_{0.03}\text{Mn}_{0.01}\text{Zn}_{0.96}\text{O}$ (inset: magnified M - H curve).

Nevertheless, the origin of ferromagnetism in ZnO is still an open debate, i.e. whether the ferromagnetism is an intrinsic property of the material or does it arise from the dopant clusters. It has been theoretically predicted by Dietl *et al* [17] that room temperature ferromagnetism can be achieved in Mn doped ZnO. Limited numbers of reports are available for the absence of ferromagnetism / AFM behaviour in TM codoped systems [9, 18, 19]. The systematic reduction in the magnetic moment with addition of Mn concentration was observed and they attributed to AFM super exchange between TM ion interactions. This is the initial report about the quenching of weak ferromagnetic behaviour in the (Ru, Mn) codoped ZnO (codoping system) and it found to be the existence of AFM interaction was observed. It is that the ferromagnetic behaviour of ZnO is quenched completely and it exhibits the antiferromagnetic behaviour. Also, leads to suppression of AFM with increasing Ru Concentration. In this scenario, no work on the variation of Ru and Mn ion in ZnO nanoparticle in an environment has come to our notice. The changes in the $M - H$ loop can be explained on the basis of the magnetic contribution from the orientation of the strong exchange interaction in the d-d couple.

The enhancement in the antiferromagnetic behaviour of (Ru, Mn) codoped ZnO may be due to the unpaired electrons in the d orbital, which is responsible for the magnetic behaviour changes. However, we suggest that Ru^{3+} ion plays an important role in the magnetic interaction. For the change in the magnetic property, the d-orbitals in the TMs may take part in the magnetic coupling. The codoping elements (i.e. Ru and Mn) are substituted in the Zn site in the ZnO lattice (Supported by XRD), the new coupling via inter ion d-d transition (3d - 4d exchange interaction) between the two dopants with free carriers causes antiferromagnetism in presence of applied magnetic field (Oe).

The another possible source for the observed magnetism is due to incorporation of trivalent Ru into divalent Mn and ZnO and also the formation of some secondary phases (supported by XRD). There is a possibility of presence of Zn interstitials and oxygen vacancies at surface of (Ru, Mn) codoped ZnO nanocrystals are responsible for the change in the magnetic property. The model proposed by Bouzerrer *et al* [20] predicts that for small potential, antiferromagnetic nearest neighbor coupling exists. As the potential increases, the coupling becomes more ferromagnetic but with further increase some couplings become antiferromagnetic again. Magnetic ions (Ru, Mn, Co, Ni ...etc.) couplings mean the decreased distance according to uncoupled states. They interact with each other's under oxygen mediation which is known as superexchange interaction (origin of antiferromagnetism).

However, the over limit (more than 5%) doping magnetic ions make all ions couple to each other, and finally the only interactions develop into the antiferromagnetic interaction [21]. We believe that, in our case, occurrence of antiferromagnetic ordering in Ru, Mn codoped ZnO nanostructures may be due to either oxygen mediated interaction or d-d coupling defects.

4. Conclusion

Nanocrystalline ZnO and (Ru, Mn) codoped ZnO were synthesized by sol – gel method via ultrasonication and their structural, optical and magnetic properties were studied. Structural and micro structural analyses were studied through XRD, HRSEM, HRTEM and the elemental compositions were determined by EDS analysis. XRD pattern of pure ZnO and (Ru, Mn) codoped ZnO shows the perfect orientation and it is evident that all the diffraction peaks can be indexed to the hexagonal wurtzite structure. There is no evidence for the formation of secondary phase upto the concentration 0.02, shows the proper incorporation of both the transition metals ie. Ru and Mn in the ZnO lattice, without altering the wurtzite structure. Further increasing concentration of Ru to 0.03 (3 mol%) formation of secondary phases of Ru as well as Mn, as RuO_2 , Mn_2O_3 , ZnMnO_3 were observed (supported by JCPDS data). The morphology of the sample was studied using HRSEM and HRTEM. It reveals from the HRSEM and HRTEM images, the powder and nano sphere like morphology was observed for pure ZnO and (Ru, Mn) codoped ZnO, respectively. The average crystallite size of the pure ZnO and (Ru, Mn) codoped ZnO are about in the range of 24-29 nm, which was in good agreement with XRD crystallite size. The selected area electron diffraction (SAED) pattern shows the hexagonal wurtzite structure. In order to understand the optical properties, UV-Vis and photoluminescence (PL) studies were carried out at room temperature. From the spectra, the defect related strong green emission peaks was observed in the visible range (460 - 480nm). The direct band gap of the as-synthesized materials are increases (3.31 eV) upto 2 mol% and then it gradually decreases (3.24 eV) on the concentration of Ru ion reaches 3 mol%. It is clearly seen from the hysteresis loop (M - H) for the nanostructures are linear with the field, indicating the anti ferromagnetism in the as-synthesized metal oxide.

5. References

- [1] Özgür Ü, Alivov Y I, Liu C, Teke A, Reshchikov M, Doğan S, Avrutin V C S J, Cho S J and Morkoc H 2005 *J. Appl. Phys.* **98**(4) 11
- [2] Sato K and Katayama-Yoshida H 2001 *Jpn. J. Appl. Phys.* **40**(4A) L334
- [3] Fukumura T, Jin Z, Kawasaki M, Shono T, Hasegawa T, Koshihara S Y and Koinuma H 2001 *Appl. Phys. Lett.* **78**(7) 958
- [4] Kumar S, Kaur P, Chen C L, Thangavel R, Dong C L, Ho Y K, Lee J F, Chan T S, Chen T K, Mok B H and Rao S M 2014 *J. Alloys Compd.* **588** 705
- [5] Ueda K, Tabata H and Kawai T 2001 *Appl. Phys. Lett.* **79**(7) 988
- [6] Neal J R, Behan A J, Ibrahim R M, Blythe H J, Ziese M, Fox A M and Gehring G A 2006 *Phys. Rev. Lett.* **96**(19) 197208
- [7] Wei Y, Hou D, Qiao S, Zhen C and Tang G 2009 *Physica B Condens. Matter* **404**(16) 2486
- [8] Vijayaprasath G, Murugan R, Asaithambi S, Sakthivel P, Mahalingam T, Hayakawa Y and Ravi G 2016 *Ceram. Int.* **42**(2) 2836
- [9] Gu Z B, Yuan C S, Lu M H, Wang J, Wu D, Zhang S T, Zhu S N, Zhu Y Y and Chen Y F 2005 *J. Appl. Phys.* **98**(5) 053908
- [10] Li H, Liu X and Zheng Z 2014 *J. Magn. Magn. Mater.* **372** 37
- [11] Sharma D and Jha R 2017 *Ceram. Int.* **43**(11) 8488
- [12] Aranganayagam K R, Senthilkumaar S, Ganapathi Subramaniam N and Kang T W 2013 *Int. J. Nanosci.* **12**(02) 1350009
- [13] Banerjee S, Rajendran K, Gayathri N, Sardar M, Senthilkumar S and Sengodan V 2008. *J. Appl. Phys.* **104**(4) 043913

- [14] Meng X, Zhao D, Shen D, Zhang J, Li B, Wang X and Fan X 2007 *J. Lumin.* **122- 123** 766
- [15] Bhosle B V, Tiwari A and Narayan J 2006 *J. Appl. Phys.* **100** 033713
- [16] Fan X M, Lian J S, Guojj Z X and Lu H J 2005 *Appl. Surf. Sci.* **239(2)** 176
- [17] Dietl T 2003 *Nat. Mater.* **2(10)** 646
- [18] Yan L, Ong C K and Rao X S 2004 *J. Appl. Phys.* **96(1)** 508
- [19] Ashokkumar M and Muthukumaran S 2015 *J. Magn. Magn. Mater.* **374** 61
- [20] Bouzerar G and Ziman T 2006 *Phys. Rev. Lett.* **96** 207602
- [21] Can M M, Fırat T and Özcan S 2011 *J. Mater Sci.* **46** 1830